Full Band Atomistic Modeling of Homo-junction InGaAs Band-to-Band Tunneling Diodes including Band Gap Narrowing

Woo-Suhl Cho[1], Mathieu Luisier[1], Dheeraj Mohata[2], Suman Datta[2], David Pawlik[3], Sean L. Rommel[3], and Gerhard Klimeck[1]

[1]*Department of Electrical and Computer Engineering, Purdue University, West Lafayette, IN 47906, USA*
[2]*Department of Electrical Engineering, The Pennsylvania State University, University Park, PA 16802, USA*
[3]*Department of Electrical and Microelectronic Engineering, Rochester Institute of Technology, Rochester, NY 14623, USA*

Abstract. A homo-junction $In_{0.53}Ga_{0.47}As$ tunneling diode is investigated using full-band, atomistic quantum transport approach based on a tight-binding model (TB) and the Non-equilibrium Green's Function formalism. Band gap narrowing (BGN) is included in TB by altering its parameters using the Jain-Roulston model. BGN is found to be critical in the determination of the current peak and the second turn-on in the forward bias region. An empirical excess current that mimics additional recombination paths must be added to the calculation to model the diode behavior in the valley current region. Overall the presented model reproduces experimental data well.

The downscaling of MOSFETs has lead to a drastic increase of power consumption, an unmanageable heat generation due to leakage currents, and a non-scalable supply voltage. Since energy efficiency is one of the biggest issues today, transistors that can help reduce the power consumption of integrated circuits and yet increase performance are highly desirable. Band-to-band tunneling field-effect transistors (TFETs) represent an attractive alternative to MOSFETs towards low voltage operations and small power consumption. In effect, they can exhibit sub-threshold swing (SS) below the kT/q limit of MOSFETs due to the injection of cold electrons. However, a sharp source to channel interface and an excellent channel electrostatic control through the gate contact are two key issues in TFETs to obtain a high ON-current and a low SS[1]. These two properties are rather difficult to obtain experimentally. On the contrary, band-to-band tunneling (BTBT) diodes can be relatively easily fabricated and offer a very good opportunity to test the tunneling properties of a given material and its potential as a TFET. Also, a thorough investigation of the underlying physics of BTBT diodes will help understanding the TFET operation, and assist the analysis of TFET design.

In BTBT diodes, current mainly flows through the junction either by tunneling or by thermionic emission. The tunneling currents depend exponentially on the energetic height and spatial width of the tunneling barrier. The desired large current densities demand rapid band bending at the tunnel junction and therefore very large doping densities. The large doping densities in turn can cause band gap narrowing (BGN), which further modulates the tunneling barrier heights. We are not aware of a study on such intricate interplay of doping densities, electrostatic potentials, and material band gaps using an atomistic full band approach. Here BGN is treated in the framework of the tight-binding (TB) approach by using the Jain-Roulston model[2], which considers the shift of the conduction and valence bands separately. BGN effects are analyzed through quantum transport simulation, and an analytically calculated excess current is added to reduce the remaining discrepancy between the experimental and simulation results around the current valley region. A homogeneous InGaAs BTBT diode lattice matched to InP and fabricated by D. Pawlik et al.[3,4] is simulated using the general-purpose quantum transport device simulator, OMEN[5] to illustrate the effectiveness of the approach presented here.

Based on the fabricated $In_{0.53}Ga_{0.47}As$ BTBT diodes[3,4] in Fig. 1(a), the one-dimensional structure in Fig. 1(b) is considered as simulation domain. An abrupt step-junction with constant doping profiles on both sides is used to model the p-n interface. An industrial standard classical drift-diffusion model, augmented by a simple tunneling model such as the Wentzel-Kramers-Brillouin (WKB) approximation requires considerable user customization to reproduce experimental data and the usage of sometimes non-physical parameter values. Furthermore, it is not predictive enough to treat tunneling devices whose behaviors are dominated by quantum mechanical effects[6]. Therefore, to investigate the I-V characteristics of the considered devices, a full-band, atomistic quantum transport simulator based on the TB model and the Non-equilibrium Green's Function (NEGF) formalism[5] is used. The sp3d5s* TB model with spin-orbit coupling is chosen for the simulation at 300K. Within the TB model the proper coupling of the conduction to the valence bands through imaginary bands is automatically included, spatial variations of the band gap and the electrostatic fields can be naturally included in the Hamiltonian construction for the quantum transport, therefore incorporating a complete non-local band-to-band tunneling model. The abrupt and dramatic changes in the doping profile effectively create a hetero-structure at

the p-n junction and a full quantum approach can properly account for the spatial modulation of the electronic charge, which cannot be modeled accurately with semi-classical models.

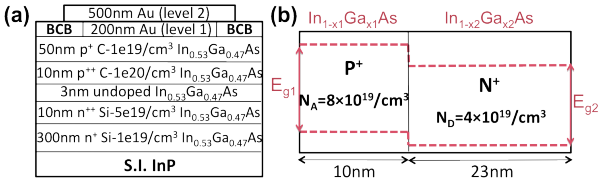

FIGURE 1. (a) The fabricated device structure[3,4] (b) The simulated structure of a InGaAs BTBT diode without (solid line) and with (dashed line) BGN.

In heavily-doped semiconductors, high impurity concentrations and small carrier-to-carrier distances increase carrier-carrier and carrier-impurity interactions. Such interactions lower the conduction band edge or raise the valence band edge of heavily-doped semiconductors and result in a net band gap reduction called band gap narrowing[7]. In BTBT diodes where both layers are heavily-doped, BGN should be taken into account since it modulates the band edges and strongly influences the magnitude of the tunneling current through the junction.

Here, the BGN at each band edge of the p- and n-sides of the diode as a function of doping concentration (N) is calculated with the Jain-Roulston model[2]. The shift of major and minority band edges (ΔE_{maj} and ΔE_{mino}, respectively) can be written as

$$\Delta E_{maj} = A\left(\frac{N}{10^{18}}\right)^{1/3} + B\left(\frac{N}{10^{18}}\right)^{1/2} \quad (1)$$

$$\Delta E_{min} = C\left(\frac{N}{10^{18}}\right)^{1/4} + D\left(\frac{N}{10^{18}}\right)^{1/2} \quad (2)$$

The parameters A, B, C, and D are derived from the material properties of p-type $In_{0.53}Ga_{0.47}As$ according to Ref. 8. For n-type, the parameters are obtained by linearly interpolating the published values for n-GaAs and the parameters extracted from experimental data for n-InAs[9]. Table I shows the parameters used for the calculation of BGN in p- and n-type $In_{0.53}Ga_{0.47}As$. The calculated band shifts as well as the total BGN are summarized in Table II.

TABLE I. BGN parameters of $In_{0.53}Ga_{0.47}As$.

Parameters	A	B	C	D
p-type	0.0092	0.0034	0.0113	0.00023
n-type	0.0476	0	0.0032	0

TABLE II. Calculated band shifts and total BGN of the device at an acceptor doping concentration of $N_A=8\times10^{19}/cm^3$ and donor concentration $N_D=4\times10^{19}/cm^3$.

Energy Band Shift [eV]	P+	N+
ΔE_{maj}	ΔE_V=0.0702	ΔE_C=0.1628
ΔE_{min}	ΔE_C=0.0358	ΔE_V=0.0079
$\Delta E_{maj}+\Delta E_{min}$	ΔE_G=0.1061	ΔE_G=0.1707

The impact of BGN is included in the quantum transport simulations by altering the TB parameters. TB parameters for $In_{1-x}Ga_xAs$ are computed by linearly interpolating the parameters of InAs and GaAs and adding a bowing parameter. Each layer of the device has an effective band gap value, depending on the local doping type and concentration. Based on the value of the reduced band gap, the In and Ga concentrations of the considered layer can be evaluated and the corresponding TB parameters are employed. The remaining band edges are illustrated in Fig. 1(b) by the dashed lines. A spatial variation in the effective alloy concentration x can mimic the BGN. An additional offset potential shifts the valence band edge to the absolute energy needed to obtain the appropriate relative shift.

In ideal BTBT diodes, for sufficiently large forward biases, energy-conserving inter-band tunneling of electrons is no longer possible and only thermally activated current flows due to the forward injection of minority carriers. However, in practice, the current at such biases is much larger than the ideally expected diode current. This difference is referred to as excess current[10]. Excess currents are typically associated with the tunneling of carriers via gap states, which originate from the band edge tails, and from imperfections such as dislocations[11]. Therefore, assuming that there are enough gap states introduced during the junction fabrication process, we should observe an excess current.

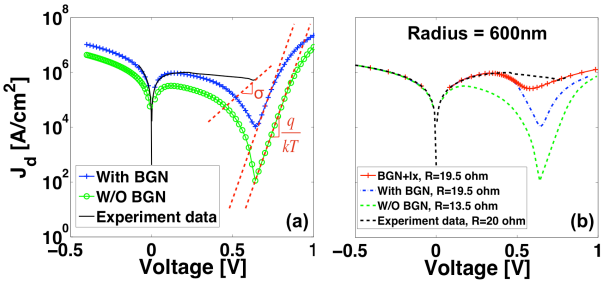

FIGURE 2. (a) Intrinsic I-V characteristics of the considered device. The simulated data with and without BGN (marked lines) are compared to the experimental data (solid line). The slopes of the currents at the valley are shown with the dotted lines. (b) Extrinsic I-V characteristics of the considered BTBT diodes. The simulated data with the effects of BGN and excess current are compared with the experimental data.

Fig. 2(a) shows the raw current data of the device without any series resistances. The thermionic current follows the equation of a normal diode and can be represented as a line with a slope close to q/kT in a semi-logarithmic plot as illustrated in Fig. 2. Although there is not enough experimental data beyond the valley, it is clear that there exists an exponential current with a much lower slope (almost 1/3 of q/kT), and few orders of magnitude higher than the conventional diode current. These facts implicate that the current at the valley is not fully thermionic. Therefore, the excess current (I_x) under forward bias must be added to the current obtained from our ballistic quantum transport simulation. This is achieved using the following equation[12]

$$I_x = I_v \exp\left[\sigma\left(V - (V_v - I_v R_s)\right)\right] \qquad (3)$$

Where I_v is the valley current at the valley voltage V_v, and R_s is a series resistance. Assuming that the excess current is dominant in the valley region, the slope of the experimental data at the valley is used to obtain the constant σ. The parameter values extracted from the raw experimental data are listed in Table III.

TABLE III. Excess current parameters.

I_v [A/cm^2]	V_v [V]	R_s [Ω·cm^2]	σ
5.164×10^5	0.745	$20(6\times10^{-5})^2\pi$	12.1

Figure 2(b) shows the effects of BGN and excess current on the simulated I-V characteristics. The series resistance is added as a post-processing step so that a good fit of the Zener tunneling current (reverse-biased side) can be obtained. Hence, the experimental Zener tunneling branch and the low forward bias range of the considered diode are well reproduced by the ballistic simulation approach including BGN. The value of the series resistance used in the simulations (19.5 Ω) is close to the experimentally estimated value of 20 Ω, and the peak current is significantly closer to the experimental data than without BGN. However, noticeable differences for the bias range after the peak current can be observed, even when BGN is included: (i) the increase of the simulated current in the negative differential resistance (NDR) region is too small, (ii) the turn-on of the thermionic current occurs at too large bias.

The enhancement of the simulated peak current is caused by BGN, which increases the tunneling current by reducing the size of the energy barrier at the junction. Also, the shifts of the majority bands pushes the Fermi levels deeper into the allowed bands, which determines the amount of tunneling current while the shift of the minority band on the p-side influences the onset of the thermionic current. Therefore, an exact calculation of each band shift is crucial to correctly estimate the current flowing through BTBT diodes.

However, purely ballistic NEGF calculations are found to be incapable to completely model BTBT diodes, and a careful investigation of the available experimental data suggests that the excess current through gap states significantly contributes to the BTBT diode current. As shown in Fig. 2(b), by including the diode excess current, the simulation data become closer to the experimental data around the valley region. While the existence of gap states partly explains the mismatch beyond the valley, further investigations are needed to determine the origin of the remaining discrepancy. The inclusion of electron-phonon scattering has been tested, but it could not increase the valley current enough to match the experimental data. Also, the BTBT diode and the measurement setup could form a kind of resonator, which changes the current magnitude. This could be another possible explanation of the discrepancy.

We conclude that in BTBT diodes, the required high impurity concentrations shift the conduction and valence band edges causing BGN, and strongly influencing the current flowing through their p-n junctions. BGN is included into an atomistic, full-band quantum transport approach by altering the TB parameters using the Jain-Roulston model. The simulated results agree well with the available experimental data in the tunneling current regions, while the inclusion of excess current improves the agreement around the valley current region.

This work is supported in part by NSF grant ECCS-0725760.

1. M. Luisier, and G. Klimeck, *IEEE Elect. Dev. Lett.* **30,** 602-604 (2009).
2. S. C. Jain, and D. J. Roulston, *Solid-State Electron.* **34**, 453-465 (1991).
3. D. Pawlik, M. Barth, P. Thomas, S. Kurinec, S. Mookerjea, D. Mohata, S. Datta, S. Cohen, D. Ritter, and S. Rommel, *Device Research Conf. Digest*, IEEE, South Bend, IN, 2010, pp. 163-164.
4. D. K. Mohata, D. Pawlik, L. Liu, S. Mookerjea, V.Saripalli, S. Rommel, and S. Datta, *Device Research Conf. Digest*, IEEE, South Bend, IN, 2010, pp. 101-102.
5. M. Luisier, A. Schenk, W. Fichtner, and G. Klimeck, *Phys. Rev. B* **74,** 205323 (2006).
6. M. Luisier, and G. Klimeck, *J. Appl. Phys.* **107,** 084507 (2010).
7. E. F. Schubert, *Doping in III-V Semiconductors*, *Cambridge*, 1993, p. 49.
8. J. M. López-González, and L. Prat, *IEEE Trans. Elect. Dev.* **44,** 1046-1051 (1997).
9. J. C. Li, M Sokolich, T. Hussain, and P. M. Asbeck, *Solid-State Electron.* **50**, 1440-1449 (2006).
10. A. G. Chynoweth, W. L. Feldmann, and R. A. Logan, *Phys. Rev* **121**, 684-694 (1961).
11. E. O. Kane, *J. Appl. Phys.* **32**, 83-91 (1961).
12. D. K. Roy, *Solid-State Electorn.* **14**, 520-523 (1971)